HHS Public Access

Author manuscript

J Mol Cell Cardiol. Author manuscript; available in PMC 2016 August 01.

Published in final edited form as:

J Mol Cell Cardiol. 2015 August ; 85: 79–88. doi:10.1016/j.yjmcc.2015.05.003.

Comparable Calcium Handling Of Human iPSC-derived Cardiomyocytes Generated By Multiple Laboratories

Hyun Seok Hwang[*,1], **Dmytro O. Kryshtal**[*,1], **Tromondae K. Feaster**[*,1], **Verónica Sánchez-Freire**[#], **Jianhua Zhang**[&], **Timothy J. Kamp**[&], **Charles C. Hong**[*], **Joseph C. Wu**[#], and **Björn C. Knollmann**[*]

[*]Division of Clinical Pharmacology, Oates Institute for Experimental Therapeutics, Vanderbilt University School of Medicine, Nashville, TN, USA

[#]Stanford Cardiovascular Institute, Stanford University School of Medicine, Stanford, CA, USA

[&]Department of Cell and Regenerative Biology, School of Medicine and Public Health, University of Wisconsin, Madison, WI, USA

Abstract

Cardiomyocytes (CMs) derived from human induced pluripotent stem cells (hiPSCs) are being increasingly used to model human heart diseases. hiPSC-CMs generated by earlier aggregation-based methods (i.e., embryoid body) often lack functional sarcoplasmic reticulum (SR) Ca stores characteristic of mature mammalian CMs. Newer monolayer-based cardiac differentiation methods (i.e., Matrigel sandwich or small molecule-based differentiation) produce hiPSC-CMs of high purity and yield, but their Ca handling has not been comprehensively investigated. Here, we studied Ca handling and cytosolic Ca buffering properties of hiPSC-CMs generated independently from multiple hiPSC lines at Stanford University, Vanderbilt University and University of Wisconsin. hiPSC-CMs were cryopreserved at each university. Frozen aliquots were shipped, recovered from cryopreservation, plated at low density and compared 3-5 days after plating with acutely-isolated adult rabbit and mouse ventricular CMs. Although hiPSC-CM cell volume was significantly smaller, cell capacitance to cell volume ratio and cytoplasmic Ca buffering were not different from rabbit-CMs. hiPSC-CMs from all three laboratories exhibited robust L-type Ca currents, twitch Ca transients and caffeine-releasable SR Ca stores comparable to adult CMs. Ca transport by sarcoendoplasmic reticulum Ca ATPase (SERCA) and Na/Ca exchanger (NCX) was similar in all hiPSC-CM lines, but slower compared to rabbit-CMs. However, the relative contribution of SERCA and NCX to Ca transport of hiPSC-CMs was comparable to rabbit-CMs. Ca handling maturity of hiPSC-CMs increased from 15 to 21 days post-induction. We conclude that hiPSC-CMs generated independently from multiple iPSC lines using monolayer-based

Correspondence to: Björn C. Knollmann, MD, PhD, Professor of Medicine and Pharmacology, Division of Clinical Pharmacology, Vanderbilt University School of Medicine, Medical Research Building IV, Rm. 1265, 2215B Garland Ave, Nashville, TN 37232-0575, Office: (615) 343-6493, Lab: (615) 936-7303, Fax: (615) 343-4522, bjorn.knollmann@vanderbilt.edu.

[1]All three first authors contributed equally

Conflict of Interest: JCW is a co-founder of Stem Cell Theranostics, all other authors declare no conflict of interest.

methods can be reproducibly recovered from cryopreservation and exhibit comparable and functional SR Ca handling.

1. Introduction

Ca signaling controls excitation-contraction coupling (ECC) in heart muscle [1]. However, detailed mechanistic studies of human cardiomyocyte (CM) Ca handling in both basic science and drug discovery have been limited by lack of an appropriate *human* CM model. The use of acutely-isolated primary human CMs is hampered by their rare availability and technical limitations. Coupled with increasing prevalence of heart failure, lack of current therapies, rising drug attrition rates and cardiac toxicity, there is a great need for in vitro human CM evaluation.

The recent establishment of human induced pluripotent stem cells (hiPSCs) has provided a new approach for obtaining human CMs [2, 3]. hiPSCs, generated from mature somatic cells harvested from patients, are analogous to human embryonic stem cells (hESCs); while avoiding the ethical controversies surrounding their use [4]. Hence, hiPSCs represent a renewable cell source of patient- or disease-specific tissue, potentially avoiding immune rejection [5]. Additionally, hiPSCs can be differentiated to cells of all three germ layers, including cardiac mesoderm [2] thus enabling generation of CMs from different genetic backgrounds. Significant progress has been made in hiPSC-CM cardiac differentiation protocols, evolving from the inefficient and variable aggregation-based methods (i.e., embryoid body (EB)), to more robust monolayer-based methods, such as the Matrigel sandwich and small molecule [6-8]. hiPSC-CMs spontaneously beat in culture, express key sarcomeric and Ca handling proteins, similar to native myocardium [7, 9]. hiPSC-CMs have been shown to recapitulate several inherited heart disease phenotypes; thus representing a theoretically unlimited source of CMs for experimental studies.

In mature ventricular CMs, ECC is initiated by membrane depolarization followed by influx of Ca via L-type Ca channels. Entering Ca triggers Ca-induced Ca release (CICR) from the sarcoplasmic reticulum (SR) via ryanodine receptor Ca release channels [10]. The ensuing rise in intracellular Ca binds to the troponin complex and activates myofilament contraction [11]. For relaxation to occur, Ca must be removed from the cytoplasm by two primary removal pathways: the sarcoendoplasmic reticulum Ca ATPase (SERCA) and the Na/Ca exchanger (NCX), with other, non-NCX non-SR removal pathways such as plasma lemma Ca ATPase and mitochondria contributing less than 5% [12]. Given Ca's central role in linking electrical activation and contraction, dysfunctional CM Ca handling has been associated with contractile dysfunction, arrhythmia and other heart diseases [13, 14].

Earlier studies of the functional properties of hiPSC-CMs have largely focused on their electrophysiological properties. hiPSC-CMs have been shown to express all ion channels naturally found in adult human left ventricular tissue [15, 16]. Additionally, hiPSC-CMs generated using the monolayer Matrigel sandwich method display human-like action potential morphology and robust L-type Ca currents [7]. However, their Ca handling properties remain not well understood. To date, Ca handling and SR function have only been investigated in hiPSC-CMs generated by the EB method [15, 17-19].

A major concern for use of hiPSC-CMs is their relatively “immature” phenotype which may result in substantial differences in their physiology when compared to native CMs. With respect to Ca handling, earlier reports have indicated that hESC-CMs and hiPSC-CMs derived from EB-based methods at times lack functional SR stores and depend primarily on trans-sarcolemmal Ca entry for contraction [9-11]. The usefulness of hiPSC-CMs depends, in part, on their contractile properties which in turn relies on Ca handling of these cells [11].

Here, we compare cell volume and intracellular Ca handling properties of hiPSC-CMs generated from multiple hiPSC lines independently by three laboratories at three different institutions to that of acutely-isolated adult rabbit and mouse ventricular CMs under identical experimental conditions. To the best of our knowledge, this is the first report of a systematic evaluation of Ca handling in hiPSC-CMs derived by monolayer based cardiac differentiation methods. We find that hiPSC-CMs from different laboratories exhibit comparable and reproducible intracellular Ca handling parameters including robust and functional SR Ca stores. We further find that both cytosolic Ca buffering properties and relative contribution of SR and sacolemmal transport pathways of hiPSC-CMs are comparable to that of acutely-isolated rabbit CMs. Taken together, our results suggest that hiPSC-CMs generated by monolayer-based methods from multiple hiPSC lines can be reproducibly recovered from cryopreservation and exhibit relatively mature Ca handling properties.

2. Material and methods

The University Committee on Use and Care of Animals at Vanderbilt University Medical Center approves all animal protocols. All animal protocols conformed to the *Guiding Principles in the Care and Use of Animals* of the American Physiological Society. Data averaged from multiple days were used for analysis. All procedures and data analysis were carried out in blinded fashion regarding the experimental groups. All chemicals, unless otherwise specified, were obtained from Sigma (St. Louis, MO).

2.1 Human iPSC Derivation and Culture

Human induced pluripotent stem cells (hiPSCs) from healthy volunteers were independently generated, as previously described, by three laboratories Stanford University [20], Vanderbilt University [21], and University of Wisconsin [7, 22]. All protocols were approved by the respective institutions Institutional Review Board. Three different methods of reprogramming were used. Briefly, the Stanford hiPSC line, 13FLVN0C1, was derived from adult fibroblast using lentivirus based reprogramming [20]. The Vanderbilt hiPSC line, CC2, was derived from dermal fibroblast by non-integrating episomal based reprogramming method [23]. The Wisconsin hiPSC line, DF19-9-11T, was derived from neonatal foreskin fibroblast by vector and transgene free episomal based reprogramming [22]. For all reprogramming individual colonies with typical hESC morphology were picked at day 17 to 30 and clonally expanded. All hiPSCs exhibit normally karyotype. hiPSC lines were routinely maintained on Matrigel, growth factor-reduced 1:200 (Corning) or on Synthemax II-SC coated plates in mTeSR1 medium (Stemcell Technologies) or E8 medium (Stanford University). Cells were passaged every 4 days using 0.5 mM EDTA (Life Technologies) in D-PBS without $CaCl_2$ or $MgCl_2$ (Life Technologies). 2 μM thiazovivin (Selleck Chemicals)

or 10 μM Rho kinase inhibitor Y-27632 (CalBiochem) was added for the first 24hrs after passaging. Cells were maintained at 37°C, with 5% CO_2 and 5% O_2.

2.2 Monolayer-Based Cardiac Differentiation

Two different protocols were used for induction of cardiac differentiation at the three institutions, both protocols yield 80-95% troponin T positive cells that spontaneously contract from day 7:

1. *Matrigel Sandwich Induction (University of Wisconsin* [7]. *& Vanderbilt University* [21]*).* Briefly, hiPSCs (>p20) were incubated with Versene solution (Invitrogen) (1 mL/well 6-well plate) at 37°C for 5 minutes to dissociate cells. Cell were seeded on Matrigel growth factor-reduced (Corning) coated plates at a density of 100,000 cells/cm^2 in mTeSR1 medium (Stemcell Technologies) supplemented with 10 μM Rho kinase inhibitor Y-27632 (CalBiochem). The mTeSR1 medium was changed daily for 4 days at which point the monolayer reached ∼80% confluence. A thin layer of Matrigel 0.5 mg was overlaid in ice-cold mTeSR1 medium. When cells reached 100% confluence, medium was changed to basal medium RPMI 1640 (11875, Life Technologies) supplemented with B-27 without insulin (Invitrogen) containing Activin A (100 ng/mL, R&D Systems) and Matrigel (0.5 mg Matrigel/6-well plate) this is referred to as day 0. On day 1 medium was changed to RPMI 1640 medium plus B-27 without insulin supplement (Invitrogen) without Matrigel and supplemented with BMP4 (5-10 ng/mL, R&D Systems) and (bFGF 5-10 ng/mL, Invitrogen) for 4 days. At day 5, RPMI 1640 medium plus B27 complete supplement (Invitrogen) was added and medium changed every 3 days until dissociation.
2. *Small Molecule Induction (Stanford University* [8, 24]*).* Briefly, hiPSCs (>p20) cultured in E8 medium were split at 1:12 ratio. Cells were grown for 4 days at which time they reached ∼80% confluence. This is referred to as day 0; medium was changed to cardiac differentiation medium consisting of RPMI 1640 (11875, Life Technologies) and B-27 minus insulin supplement (A1895601, Life Technologies) supplemented with 10 μM CHIR99021 (LC Laboratories) for day 0 to day 1. On day 1 medium was changed to cardiac differentiation medium. On day 3 medium was changed to cardiac differentiation medium supplemented with 5 μM IWR-1 (Sigma). On day 5 medium was changed to cardiac differentiation medium. Medium was changed on day 7 to cardiac medium consisting of RPMI1640 (11875, Life Technologies) and B-27 supplement (17504, Life Technologies), and every other day until dissociation.

2.3 hiPSC-CM dissociation, storage and plating

hiPSC-CMs were incubated with TrypLE Express (Life Technologies) for 10 minutes at 37°C to dissociated cells. hiPSC-CMs were cryopreserved in 10% DMSO, 90% FBS and stored in liquid nitrogen at day 15, 21, and 30 after cardiac induction. For experimental studies, hiPSC-CMs were thawed and plated at low density on Matrigel growth factor-reduced coated dishes in solution containing: RPMI 1640 medium (11875, Life Technologies), 2% B-27 supplement (Invitrogen), and 1% Pen-Strep (Life Technologies).

hiPSC-CMs were maintained at 5% CO_2 and 21% O_2. All experiments were performed 3-5 days after plating.

2.4 Primary Myocyte Isolation

Ventricular myocytes from mouse and rabbit were isolated by a modified collagenase/protease method as previously described [25]. All the experiments conducted in Tyrode's solution containing (in mM): $CaCl_2$, NaCl 134, KCl 5.4, $MgCl_2$ 1, glucose 10, and HEPES 10, pH adjusted to 7.4 with NaOH. Final concentration of Ca is 2 mM.

2.5 Measurement of cell volume

To measure myocyte volume, Z-stacks were obtained using a confocal microscope (LSM 510, 25× oil immersion Plan-Neofluar lens) as described in [26]. Briefly, myocytes were loaded with Calcein AM (5 μM, 30 min; Molecular Probes, Eugene, OR) to label intracellular space. Myocytes were washed twice to remove extracellular calcein. Calcein fluorescence was excited at 488-nm with 1% argon laser power. 25-46 images (1.5 μm sections) were obtained for each myocytes. Images were reconstructed in 3D and surface area and volume analyzed using the 3D image analysis program IMARIS (Bitplane, South Windsor, CT).

2.6 Measurement of Intracellular Ca

Myocytes were loaded with Fura-2 acetoxymethyl ester, Fura-2 AM (Molecular Probes Inc, Eugene, OR) as described previously [25]. Briefly, myocytes were incubated with 2 μM Fura 2 AM for 8 minutes at room temperature to load the indicator in the cytosol. Myocytes were washed twice for 10 minutes with Tyrode's solution containing 250 μM probenecid to retain the indicator in the cytosol. A minimum of 30 min were allowed for de-esterification before imaging the cells. Fura 2-AM loaded myocyte Ca transients recorded during 0.5 Hz field stimulation in 2 mM Ca Tyrode's solution for 20 second at room temperature. Then stimulation was switched off followed by application of caffeine 10 mM for 5 second to estimate SR Ca content. A subset of cells were exposed to 0Ca0Na Tyrode's solution for 10 second then caffeine 10 mM applied for 30 second to estimate non-NCX Ca extrusion. For each cell and each experimental condition, tau (τ), amplitude and baseline values were averaged from 3 consecutive Ca transients. Ca transients were recorded and analyzed using commercially available data analysis software (IonOptix, IonWizardTM Milton, MA). All experiments were conducted at room temperature.

2.7 Ca buffering measurements

To measure cytosolic Ca buffering, we used the “Trafford” method [27], as described in detail in [28]. Briefly, myocytes were loaded with 25 μM Fluo-4 salt into pipette solution to measure cytosolic Ca. Caffeine (10 mM) was rapidly applied to release Ca from the SR, which then extruded via the Na/Ca exchanger (NCX), generating an inward NCX current. Integration of NCX current yielded the total amount of Ca released from the SR. To calculate Ca concentration, cell volume was estimated from the cell capacitance using the published conversion factor of 4.58 pF/pL for rabbit CM. The conversion factor of 4.57 pF/pL for hiPSC-CM was calculated from the average hiPSC-CM volume of based on the

measured average hiPSC-CM volume of 3.96±0.25 pL (Fig. 1) and average hiPSC-CM capacitance of 18.1 ±1.4 pF. Then $\Delta[ca]_{total}$ was plotted as a function of $\Delta[ca]_{free}$ and maximal cytosolic buffering capacity (B_{max}) and dissociation constant (K_d) calculated. For consistency, cellular Ca is represented in units of μmol/$L_{cytosol}$, excluding mitochondrial contribution [29].

2.8 Measurements of L-type Ca current

Mouse-CM and iPSC-CMs were studied using whole-cell patch clamp technique. External solution contained (in mM): NaCl 134, CsCl 5, $MgCl_2$ 1, $CaCl_2$ 2, glucose 10, HEPES 10, adjusted to pH 7.4 with NaOH. The pipette solution contained (in mM): CsCl 110, $MgCl_2$ 1, MgATP 5, cAMP 0.2; EGTA 14; Hepes 20; adjusted to pH=7.25 with CsOH. Currents were elicited by 200-ms depolarizing steps ranging from -40 mV to +40 mV (with 10 mV increment), from holding potential of -70 mV. A 20-ms conditioning pulse to -40 mV was applied prior to test pulse to inactivate Na currents. All experiments were carried out at room temperature.

2.9 Calculation of Ca flux balance

The decay rates of Ca transients in different extracellular solutions were used to calculate relative contribution of Ca removal pathways during relaxation in myocytes [29]. Briefly, total Ca removal from the cytosol was estimated by the rate constant of field-stimulated twitch Ca transients (τ_{twitch}). The rate constant of caffeine-induced Ca transient (τ_{Caff}) represents non-SR Ca removal pathways (caffeine opens SR Ca release channels and prevents SR Ca uptake), which in cardiomyocytes is primarily the NCX. The rate constant of caffeine-induced Ca transient in Na and Ca-free solutions ($\tau_{Caff0Na}$), which blocks the NCX, measures non-NCX non SR-mediated Ca removal. The relative contribution of each Ca flux pathway was calculated from removal time constant τ (s) of Ca transients for the three different conditions, with the following equations:

$$1/\tau_{\text{twitch}} = K_{\text{SERCA}} + K_{\text{NCX}} + K_{\text{non-NCX}} \quad (1)$$

$$1/\tau_{\text{Caff}} = K_{\text{NCX}} + K_{\text{non-NCX}} \quad (2)$$

$$1/\tau_{\text{Caff0Na}} = K_{\text{non-NCX}} \quad (3)$$

K_{SERCA}, K_{NCX} and $K_{non\text{-}NCX}$ represent the rates of Ca uptake into the SR, NCX-mediated removal and non-NCX non-SR mediated removal, respectively.

2.10 Statistical analysis

Differences among the groups were assessed using one-way ANOVA. Results were considered statistically significant if the p-value was less than 0.05 adjusted by Bonferroni correction for multiple comparisons.

3. Results

3.1 Cell morphometry and Ca handling of hiPSC-CMs and adult ventricular animal-CMs

Single hiPSC-CMs at age 21 days post induction were plated at low density on Matrigel coated dishes and cell surface area, cell volume and Ca handling measured 3-5 days after plating. Protein expression, CM purity, and electrophysiological characterization of the hiPSC-CMs used in our experiments have been reported elsewhere [7, 8, 21] and are not investigated here. We first measured myocyte shape and volume from Z-stacks of confocal images after loading cells with calcein to label intracellular space [26]. The shape of hiPSC-CM was highly variables, ranging from circular to elongated to triangular morphology (Fig. 1A). hiPSC-CMs were much smaller (cell volume 3.96±0.25 pL, n=44) compared to adult mouse ventricular CM (cell volume 29±2 pL, n=34). On the other hand, cell surface area to volume ratio was significantly larger in hiPSC compared to mouse CM (Fig. 1B). Circular hiPSC-CM had lower surface area and volume compared to elongated and triangular iPSC-CM, but surface to volume ratio was not statistically different among the three hiPSC-CM cell shapes (Fig. 1B).

Despite the differences in cell size and shape, staining with the low-affinity Ca sensitive indicator Mag Fluo-4 demonstrates that both hiPSC-CMs and adult mouse-CMs have robust intracellular Ca stores (Fig. 2A). We next compared the Ca handling of field-stimulated (0.5Hz) hiPSC-CMs to that of adult primary ventricular rabbit and mouse CMs under identical experimental conditions. Typical Ca handling parameters (diastolic [ca], Ca transient amplitude, time to peak, Ca decay rate) were not significantly different among all three hiPSC-CM lines. Compared to adult rabbit and mouse CMs, only time to peak and Ca transient decay rates were significantly slower in hiPSC-CM, whereas all other Ca handling parameters were not different (Fig. 2).

We next tested for the presence of functional sarcoplasmic reticulum (SR) Ca stores using caffeine, an agonist of ryanodine receptor (RyR2) Ca release channels. Analogous to adult primary CMs, all hiPSC-CMs tested exhibited robust caffeine-releasable SR Ca stores (Fig. 2 B&C). Caffeine-induced Ca transients and hence SR Ca content were of similar magnitude and not significantly different from rabbit or mouse-CMs. These results are consistent with the presence of intracellular Ca stores stained with Mag Fluo-4 (Fig. 2A) Taken together; these data demonstrate that single hiPSC-CMs exhibit intracellular Ca transients comparable to that of adult animal-CMs, and that the presence of functional SR in hiPSC-CMs derived using monolayer-based methods is consistent across multiple labs.

3.2 Cytoplasmic Ca buffering characteristics of hiPSC-CMs and rabbit-CMs

Using the height of the caffeine-induced Ca transient (Fig. 2) as measure of SR Ca content assumes that cytoplasmic buffering is unchanged; an assumption that may not be correct because hiPSC-CMs display disorganized contractile filaments [18], Ca binding to myofilaments accounts for a large proportion of cytosolic Ca buffering [29]. Nevertheless, hiPSC-CMs studied here exhibit robust expression of myofilament proteins, including troponin C [16], the latter being the functionally most important cytosolic Ca buffering site during physiological ECC [29]. Hence, we measured the cytoplasmic Ca buffering capacity

of hiPSC-CMs using the Trafford method (Fig. 3 A). Although hiPSC-CMs were significantly smaller than rabbit-CMs (cell capacitance 18±1 pF vs 101±12 pF, $p<0.01$), the average cell capacitance to cell volume ratio of hiPSC-CM was 4.46 pF/pL, a value that is very close to the published value for rabbit ventricular myocytes (4.47 pF/pL) [26]. Maximal binding capacity B_{max}, which is an estimate of the total cytoplasmic Ca binding sites, was not significantly different between hiPSC-CMs and rabbit CMs (Fig. 3B, top panel). Likewise, the apparent dissociation constant K_d, an estimate of the cytosolic Ca binding affinity, was not significantly different between hiPSC-CMs and rabbit-CMs (Fig. 3B, lower panel). These results demonstrate that multiple hiPSC-CM lines have comparable cytosolic Ca buffering properties which are comparable to those of acutely-isolated rabbit-CMs.

3.3 Characterization of Ca fluxes in hiPSC-CMs

During each contraction-relaxation cycle, Ca enters the cytosol via L-type Ca channels and via Ca-induced Ca release from SR Ca stores. Consistent with their robust twitch Ca transients (Fig. 2), all three hiPSC-CM lines exhibit robust L-type Ca currents that were not statistically different from L-type Ca current measured in mouse CM (Fig. 4). Cytoplasmic Ca removal is mediated by three major pathways: (1) Ca uptake into the SR by the sarcoendoplasmic reticulum CaATPase (SERCA), (2) Ca efflux from the cell via the NCX, and (3), non-NCX non-SR mediated pathways such as plasma lemma Ca ATPase and mitochondria [25, 29]. The contribution of the individual Ca removal mechanisms has been studied extensively in non-human CMs [30, 31] but not yet in hiPSC-CMs. SR-independent Ca removal was tested by rapid caffeine application and was significantly slower in hiPSC-CMs compared to rabbit and mouse CMs (Fig. 5A). Block of NCX by 0Na 0Ca abolished the differences between hiPSC-CMs and animal CMs (Fig. 5B), suggesting that NCX-mediated Ca transport was responsible for the difference. We next used the flux balance method to calculate transport rate constants for SERCA, NCX and non-NCX. Compared to rabbit-CMs, Ca flux via SERCA was significantly slower in the hiPSC-CMs, and significantly faster in mouse-CMs (Supplemental Table 1). NCX Ca transport was also slower in hiPSC-CMs compared to mouse and rabbit CMs, whereas non NCX Ca removal was similar in all groups (Supplemental Table 1).

Next, we calculated the *relative* contribution of the Ca removal pathways from the individual decay rate constants listed in supplemental table 1. Relative contribution of the three Ca transport systems (SERCA, NCX, non-NCX) was comparable in all three hiPSC-CM lines (Fig. 6). Furthermore, contribution of SERCA (61%) and NCX (31%) in hiPSC-CMs was not significantly different from adult rabbit-CMs (SERCA 60%, NCX 32%). As expected [29, 30], SERCA (89%) dominated in mouse-CMs. On the other hand, the relative contribution of non-NCX removal pathways was significantly larger in hiPSC-CMs (8-9%) compared to rabbit-CMs (4%) and mouse-CMs (2%).

3.4 Maturation of hiPSC-CMs Ca handling

Time in culture greatly affects molecular profile, morphology and function of hiPSC-CMs [32]. However, the time dependence of Ca handling maturation has not been studied. Hence, we examined Ca handling at three times after induction of cardiac differentiation (day 15, 21, and 30). Day 15 hiPSC-CMs exhibited significantly smaller Ca twitch transients (F_{ratio},

τ_{twitch}, day 15, 0.27±0.07*; day 21, 0.40±0.09; day 30, 0.41±0.07, *P<0.05 vs day 21) and ~40% lower SR Ca content compared to day 21 hiPSC-CMs (Fig. 7A). No further changes were observed in day 30 hiPSC-CM. Next, we investigated the time dependence of changes in Ca flux pathways in more detail. The average decay time constants of Ca twitch transients (τ_{twitch}) was significantly slower in day 15 hiPSC-CMs compared with that of day 21 or day 30 hiPSC-CMs (Fig. 7B). Likewise, caffeine-induced Ca transients were also significantly slower in day 15 hiPSC-CMs compared with that of day 21 or day 30 (τ_{Caff} (s): day 15, 5.0±0.4*; day 21, 2.9±0.4; day 30, 3.0±0.2, *P<0.05). However, non-NCX and non-SR mediated Ca removal time constants were not affected by longer time in culture after cardiac induction ($\tau_{Caff0Na}$ (s): day 15, 14.9±1.7; day 21, 14.3±2.1; day 30, 12.9±0.8). These data demonstrate that the absolute rates of Ca transport via SERCA and NCX significantly increase between day 15 and day 21 hiPSC-CMs, whereas Ca fluxes via non-SR and non-NCX mechanisms remain relatively constant. As a result, the relative contribution of Ca flux pathways shifts to predominantly SERCA and NCX (Fig. 7C), as seen in adult rabbit CMs (Fig. 6). Hence, relativity mature Ca handling properties are reached as early as day 21 post cardiac differentiation.

To evaluate the reproducibility of hiPSC-CMs Ca handling measurements, we quantified Ca flux parameters in hiPSC-CMs (21 days post cardiac induction) from the same cryopreserved batch that were plated on different days. The average decay rates of twitch and caffeine-induced Ca transients were not significantly different between two independent plating for all three hiPSC-CM lines (Fig. 8A). Furthermore, the relative contribution of Ca transport pathways was almost identical in each batch (Fig. 8B). These results demonstrate that intracellular Ca handling measurements are consistent and reproducible across multiple independently generated hiPSC-CM lines.

4. Discussion

4.1 Ca handling of hiPSC-CMs

Our report is the first study that systematically quantifies Ca fluxes in hiPSC-CMs. Major new findings are that hiPSC-CMs generated by the latest monolayer based cardiac differentiation protocols exhibit robust and functional SR Ca handling, and that the relative contribution of SR Ca flux (60%) in hiPSC-CMs is not statistically different from that of acutely-isolated adult rabbit ventricular CMs (Fig. 6). Moreover, we have for the first time quantified cytosolic Ca buffering in hiPSC-CMs, which is comparable to that of rabbit-CMs (Fig. 3). The latter result is of critical importance for interpreting results from experiments using fluorescent Ca indicators in CMs [33], an approach that is widely used for measuring Ca transients and SR Ca content. Finally, our results demonstrate that independently generated hiPSC-CM lines from healthy donors exhibit comparable and reproducible Ca handling and cytosolic Ca buffering properties.

Previous studies of hESC-CMs and hiPSC-CMs generated by aggregation-based methods (e.g., EB method) reported either a complete lack of caffeine-releasable SR Ca stores [9] or their presence only in a sub-population of CMs [18, 19, 34, 35]. One study finds hiPSC-CMs Ca handling relatively immature compared to hESC-CMs. In contrast, we find caffeine-release Ca stores in essentially 100% of hiPSC-CMs tested, which is the same as in acutely-

isolated adult CMs. The reasons for these differences are unclear, but could be due to cardiac differentiation variability, dependence on chemically undefined growth factors and cytokines, or growth factors and cytokines failing to gain access to the EB interior. Given that the two monolayer approaches of cardiac induction used here are standardized and published, and that Ca handling parameters at 21 days post induction (Fig. 2) was comparable among hiPSC-CMs generated independently in difference labs, these two monolayer methods may be preferable for future studies using hiPSC-CMs as cardiac disease models. A recent report also characterized Ca handling of hiPSC-CMs generated by monolayer-based Matrigel Sandwich method [36]. However, this study only evaluated twitch Ca amplitude and morphology in response to different pacing rates, while SR function and Ca fluxes were not evaluated. Furthermore, Ca fluorescence measurements were obtained from clumps or clusters of cells, not single cells as in our study. These cases highlight the discrepancies in the field, the need for proper Ca handling controls, and consistent experimental design to compare results.

4.2 Comparison of hiPSC-CMs and acutely-isolated adult CMs

Lacking access to acutely-isolated healthy human ventricular CMs – a common problem for the field – we compared hiPSC-CMs with rabbit and mouse CMs. Ca handling of rabbit-CMs are thought to be similar to that of human ventricular CMs and have been widely used to model human heart diseases [10]. We found that hiPSC-CMs have twitch transient amplitude, resting diastolic Ca and SR Ca content that are comparable to that of rabbit-CMs. This contrasts with previous reports indicating that hiPSC-CMs have smaller relatively “immature” Ca transients [11]. On the other hand, two main differences exist between hiPSC and rabbit CM Ca handling: 1) significantly slower SERCA and NCX Ca transport (supplemental table 1) and 2) slower time to peak Ca transient (Fig. 2). Factors such as the lack of t-tubules of hiPSC-CMs leading to an inefficient Ca induced Ca release and hence impaired Ca-dependent inhibition of L-type Ca current during the action potential plateau may contribute to the slower time to peak of hiPSC-CM Ca transients. While the differences in SERCA and NCX function could be due to species differences between human and rabbits, a more likely explanation is that Ca transport remains somewhat immature in hiPSC-CMs compared to adult CMs. It will be interesting to study Ca fluxes in hiPSC-CMs generated using approaches that reportedly increase hiPSC-CM maturity (e.g., 2D patterning [37], electrical stimulation [38], 3D culture methods [39]). For example, Rao et al. reported a faster time to peak and better SR function of hiPSC-CMs cultured on microgrooved compared to unstructured polydimethylsiloxane membranes [37].

4.3 Maturation hiPSC-CM Ca handling

Although hiPSC-CMs beat as early as day 7 after cardiac induction, significant changes occur as the hiPSC-CMs continue to develop. For example, hiPSC-CMs day 10 to 15 post-induction were shown to exhibit decreased contractile response compared to older hiPSC-CMs [40]. Therefore, we investigated Ca handling at day 15, 21, and 30 after cardiac induction. We found that day 15 hiPSC-CMs exhibit decreased twitch Ca transients and SR Ca stores compared to day 21 hiPSC-CMs. Interestingly, hiPSC-CMs did not continue to mature their Ca handling from day 21 to 30 (Fig. 7A). The flux balance analysis showed a temporal transition of Ca flux contributions from day 15 to day 21, with SERCA and NCX

contribution remaining similar, while non-NCX contribution is decreased in day 21 hiPSC-CMs. These results suggest that non-NCX pathways may be compensating for the decreased SECA activity in early stage hiPSC-CMs. An earlier study [34] reported that NCX is largely responsible for maintaining Ca homeostasis in hESC-CMs and that genetic transfer may be necessary to increase SERCA contribution. However, our results demonstrate that in hiPSC-CMs this is not the case.

4.4 Implications for future hiPSC studies

The results of our experiments have a number of implications for using hiPSC-CMs as experimental models. (1) hiPSC-CMs should be allowed to mature in culture for at least 21 days instead of using when the initially start beating [34, 41]. (2) To reduce variability of the results, hiPSC should be studied at a narrow and defined time window after induction instead of the wide windows of day 7-50 utilized previously [41]. (3) Monolayer-based methods of cardiac differentiation are capable of generating hiPSC-CM with robust and functional SR Ca stores. (4) Our experimental results provide a foundation for future disease modeling studies by elucidating what “normal” hiPSC-CM Ca handling is in vitro. (5) hiPSC-CMs can be reproducibly recovered from cryopreservation demonstrating that these cells exhibit robust reproducible properties especially with regard to Ca cycling. (6) hiPSC-CMs made from different hiPSC lines that were derived from different tissue sources by different methods of reprogramming have comparable Ca handling. This result is reassuring, since there is concern in the field that starting cell source, e.g. neonatal or adult fibroblast, and reprogramming methodology, e.g. lentivirus- or episomal- based may impact differentiated cell progeny, e.g. alter ECC, our result demonstrate starting somatic cell source does not clearly impact functional readout. Further, reprogramming methodology also does not obviously impact progeny function. We show here in a direct comparison under identical experimental conditions that hiPSC-CMs from fully reprogrammed hiPSCs using different cell sources and reprogramming methodologies by different laboratories yield comparable results.

Finally, the methods of cryopreservation and recovery described here could serve as a first step of standardization, which is greatly needed in the field. Having frozen stocks of hiPSC-CM that can be reproducibly recovered as shown here opens up a number of possibilities. Cells can be shared between labs, saved for future experiments, or for doing larger experiments such as screening compound libraries.

4.5 Limitations

Our study has several limitations. To ensure identical study conditions, all hiPSC-CMs were frozen at specific dates after cardiac differentiation, then thawed and re-plated prior to study. We cannot exclude that the freezing and thawing process has altered the phenotype of the hiPSC-CMs. However, the advantage of this approach is that multiple batches of re-plated cells from different labs can be readily compared, which is why we chose this approach here. This is also the reason why we could not examine hiPSC-CMs older than 30 days, because the viability of older cells decreases substantially after freezing. Another limitation is that we did not differentiate hiPSC-CM subtype (i.e., nodal, atrial, and ventricular-like). However, previous studies have shown that the cardiac induction protocols used here

produce approximately 80% ventricular-like CMs. Importantly, the cell to cell variability of Ca handling parameters (i.e., twitch transient amplitude) of hiPSC-CMs was comparable to that of acutely-isolated adult CMs (approximately a 30% coefficient of variation, see Fig. 2). Finally, we did not tested whether our hiPSC-CMs also have prominent inositol triphosphate (IP3) sensitive intracellular Ca stores as previously reported for hESC-CMs. These Ca stores are not thought to play a role in healthy adult ventricular CMs physiology however they can be upregulated in diseased myocytes [42]. Future studies will have to determine if IP3 Ca stores are present, and what effects if any they have on steady-state Ca handling in hiPSC-CMs derived from healthy volunteers.

Supplementary Material

Refer to Web version on PubMed Central for supplementary material.

Acknowledgments

None

Funding: This work was partly supported by the United States National Institutes of Health [HL88635, HL71670 & HL108173 to B.C.K.; NIH HL104040 to C.C.H.]; by the American Heart Association [13IRG13680003 to B.C.K., 12SDG12050597 to H.S.H., 12POST12080080 to D.K.], and by the Veterans Administration Merit Grant BX000771 to C.C.H.

References

1. Jafri MS. Models of excitation-contraction coupling in cardiac ventricular myocytes. Methods Mol Biol. 2012; 910:309–35. [PubMed: 22821602]
2. Takahashi K, Yamanaka S. Induction of pluripotent stem cells from mouse embryonic and adult fibroblast cultures by defined factors. Cell. 2006; 126:663–76. [PubMed: 16904174]
3. Takahashi K, Okita K, Nakagawa M, Yamanaka S. Induction of pluripotent stem cells from fibroblast cultures. Nat Protoc. 2007; 2:3081–9. [PubMed: 18079707]
4. Knollmann BC. Induced pluripotent stem cell-derived cardiomyocytes: boutique science or valuable arrhythmia model? Circ Res. 2013; 112:969–76. discussion 76. [PubMed: 23569106]
5. Yamanaka S. Strategies and new developments in the generation of patient-specific pluripotent stem cells. Cell Stem Cell. 2007; 1:39–49. [PubMed: 18371333]
6. Laflamme MA, Chen KY, Naumova AV, Muskheli V, Fugate JA, Dupras SK, et al. Cardiomyocytes derived from human embryonic stem cells in pro-survival factors enhance function of infarcted rat hearts. Nat Biotechnol. 2007; 25:1015–24. [PubMed: 17721512]
7. Zhang J, Klos M, Wilson GF, Herman AM, Lian X, Raval KK, et al. Extracellular matrix promotes highly efficient cardiac differentiation of human pluripotent stem cells: the matrix sandwich method. Circ Res. 2012; 111:1125–36. [PubMed: 22912385]
8. Burridge PW, Matsa E, Shukla P, Lin ZC, Churko JM, Ebert AD, et al. Chemically defined generation of human cardiomyocytes. Nat Methods. 2014; 11:855–60. [PubMed: 24930130]
9. Yang X, Pabon L, Murry CE. Engineering adolescence: maturation of human pluripotent stem cell-derived cardiomyocytes. Circ Res. 2014; 114:511–23. [PubMed: 24481842]
10. Bers DM. Cardiac excitation-contraction coupling. Nature. 2002; 415:198–205. [PubMed: 11805843]
11. Lee YK, Ng KM, Lai WH, Chan YC, Lau YM, Lian Q, et al. Calcium homeostasis in human induced pluripotent stem cell-derived cardiomyocytes. Stem Cell Rev. 2011; 7:976–86. [PubMed: 21614516]
12. Fearnley CJ, Roderick HL, Bootman MD. Calcium signaling in cardiac myocytes. Cold Spring Harb Perspect Biol. 2011; 3:a004242. [PubMed: 21875987]

13. O'Rourke B, Kass DA, Tomaselli GF, Kääb S, Tunin R, Marbán E. Mechanisms of altered excitation-contraction coupling in canine tachycardia-induced heart failure, I: experimental studies. Circ Res. 1999; 84:562–70. [PubMed: 10082478]

14. Pogwizd SM, Qi M, Yuan W, Samarel AM, Bers DM. Upregulation of Na(+)/Ca(2+) exchanger expression and function in an arrhythmogenic rabbit model of heart failure. Circ Res. 1999; 85:1009–19. [PubMed: 10571531]

15. Itzhaki I, Rapoport S, Huber I, Mizrahi I, Zwi-Dantsis L, Arbel G, et al. Calcium handling in human induced pluripotent stem cell derived cardiomyocytes. PLoS One. 2011; 6:e18037. [PubMed: 21483779]

16. Liang P, Lan F, Lee AS, Gong T, Sanchez-Freire V, Wang Y, et al. Drug screening using a library of human induced pluripotent stem cell-derived cardiomyocytes reveals disease-specific patterns of cardiotoxicity. Circulation. 2013; 127:1677–91. [PubMed: 23519760]

17. Lan F, Lee AS, Liang P, Sanchez-Freire V, Nguyen PK, Wang L, et al. Abnormal calcium handling properties underlie familial hypertrophic cardiomyopathy pathology in patient-specific induced pluripotent stem cells. Cell Stem Cell. 2013; 12:101–13. [PubMed: 23290139]

18. Sun N, Yazawa M, Liu J, Han L, Sanchez-Freire V, Abilez OJ, et al. Patient-specific induced pluripotent stem cells as a model for familial dilated cardiomyopathy. Sci Transl Med. 2012; 4:130ra47.

19. Zhang GQ, Wei H, Lu J, Wong P, Shim W. Identification and characterization of calcium sparks in cardiomyocytes derived from human induced pluripotent stem cells. PLoS One. 2013; 8:e55266. [PubMed: 23408964]

20. Sharma A, Marceau C, Hamaguchi R, Burridge PW, Rajarajan K, Churko JM, et al. Human induced pluripotent stem cell-derived cardiomyocytes as an in vitro model for coxsackievirus B3-induced myocarditis and antiviral drug screening platform. Circ Res. 2014; 115:556–66. [PubMed: 25015077]

21. Yang T, Chun YW, Stroud DM, Mosley JD, Knollmann BC, Hong C, et al. Screening for Acute IKr Block Is Insufficient to Detect Torsades de Pointes Liability: Role of Late Sodium Current. Circulation. 2014; 130:224–34. [PubMed: 24895457]

22. Yu J, Hu K, Smuga-Otto K, Tian S, Stewart R, Slukvin II, et al. Human induced pluripotent stem cells free of vector and transgene sequences. Science. 2009; 324:797–801. [PubMed: 19325077]

23. Okita K, Matsumura Y, Sato Y, Okada A, Morizane A, Okamoto S, et al. A more efficient method to generate integration-free human iPS cells. Nat Methods. 2011; 8:409–12. [PubMed: 21460823]

24. Sanchez-Freire V, Lee AS, Hu S, Abilez OJ, Liang P, Lan F, et al. Effect of human donor cell source on differentiation and function of cardiac induced pluripotent stem cells. J Am Coll Cardiol. 2014; 64:436–48. [PubMed: 25082575]

25. Knollmann BC, Chopra N, Hlaing T, Akin B, Yang T, Ettensohn K, et al. Casq2 deletion causes sarcoplasmic reticulum volume increase, premature Ca2+ release, and catecholaminergic polymorphic ventricular tachycardia. J Clin Invest. 2006; 116:2510–20. [PubMed: 16932808]

26. Satoh H, Delbridge LM, Blatter LA, Bers DM. Surface:volume relationship in cardiac myocytes studied with confocal microscopy and membrane capacitance measurements: species-dependence and developmental effects. Biophys J. 1996; 70:1494–504. [PubMed: 8785306]

27. Trafford AW, Diaz ME, Eisner DA. A novel, rapid and reversible method to measure Ca buffering and time-course of total sarcoplasmic reticulum Ca content in cardiac ventricular myocytes. Pflugers Arch. 1999; 437:501–3. [PubMed: 9914410]

28. Schober T, Huke S, Venkataraman R, Gryshchenko O, Kryshtal D, Hwang HS, et al. Myofilament Ca sensitization increases cytosolic Ca binding affinity, alters intracellular Ca homeostasis, and causes pause-dependent Ca-triggered arrhythmia. Circ Res. 2012; 111:170–9. [PubMed: 22647877]

29. Bers DM. Calcium fluxes involved in control of cardiac myocyte contraction. Circ Res. 2000; 87:275–81. [PubMed: 10948060]

30. Puglisi JL, Goldspink PH, Gomes AV, Utter MS, Bers DM, Solaro RJ. Influence of a constitutive increase in myofilament Ca(2+)-sensitivity on Ca(2+)-fluxes and contraction of mouse heart ventricular myocytes. Arch Biochem Biophys. 2014; 552-553:50–9. [PubMed: 24480308]

31. Berlin JR, Bassani JW, Bers DM. Intrinsic cytosolic calcium buffering properties of single rat cardiac myocytes. Biophys J. 1994; 67:1775–87. [PubMed: 7819510]
32. Lundy SD, Zhu WZ, Regnier M, Laflamme MA. Structural and functional maturation of cardiomyocytes derived from human pluripotent stem cells. Stem Cells Dev. 2013; 22:1991–2002. [PubMed: 23461462]
33. Diaz ME, Trafford AW, Eisner DA. The role of intracellular Ca buffers in determining the shape of the systolic Ca transient in cardiac ventricular myocytes. Pflugers Arch. 2001; 442:96–100. [PubMed: 11374074]
34. Liu J, Fu JD, Siu CW, Li RA. Functional sarcoplasmic reticulum for calcium handling of human embryonic stem cell-derived cardiomyocytes: insights for driven maturation. Stem Cells. 2007; 25:3038–44. [PubMed: 17872499]
35. Dolnikov K, Shilkrut M, Zeevi-Levin N, Gerecht-Nir S, Amit M, Danon A, et al. Functional properties of human embryonic stem cell-derived cardiomyocytes: intracellular Ca2+ handling and the role of sarcoplasmic reticulum in the contraction. Stem Cells. 2006; 24:236–45. [PubMed: 16322641]
36. Riedel M, Jou CJ, Lai S, Lux RL, Moreno AP, Spitzer KW, et al. Functional and pharmacological analysis of cardiomyocytes differentiated from human peripheral blood mononuclear-derived pluripotent stem cells. Stem Cell Reports. 2014; 3:131–41. [PubMed: 25068127]
37. Rao C, Prodromakis T, Kolker L, Chaudhry UA, Trantidou T, Sridhar A, et al. The effect of microgrooved culture substrates on calcium cycling of cardiac myocytes derived from human induced pluripotent stem cells. Biomaterials. 2013; 34:2399–411. [PubMed: 23261219]
38. Chan YC, Ting S, Lee YK, Ng KM, Zhang J, Chen Z, et al. Electrical stimulation promotes maturation of cardiomyocytes derived from human embryonic stem cells. J Cardiovasc Transl Res. 2013; 6:989–99. [PubMed: 24081385]
39. Eschenhagen T, Fink C, Remmers U, Scholz H, Wattchow J, Weil J, et al. Three-dimensional reconstitution of embryonic cardiomyocytes in a collagen matrix: a new heart muscle model system. FASEB J. 1997; 11:683–94. [PubMed: 9240969]
40. Germanguz I, Sedan O, Zeevi-Levin N, Shtrichman R, Barak E, Ziskind A, et al. Molecular characterization and functional properties of cardiomyocytes derived from human inducible pluripotent stem cells. J Cell Mol Med. 2011; 15:38–51. [PubMed: 20041972]
41. Dolnikov K, Shilkrut M, Zeevi-Levin N, Danon A, Gerecht-Nir S, Itskovitz-Eldor J, et al. Functional properties of human embryonic stem cell-derived cardiomyocytes. Ann N Y Acad Sci. 2005; 1047:66–75. [PubMed: 16093485]
42. Roderick HL, Knollmann BC. Inositol 1,4,5-trisphosphate receptors: “exciting” players in cardiac excitation-contraction coupling? Circulation. 2013; 128:1273–5. [PubMed: 23983251]

Highlights

- We studied Ca handling and cytosolic Ca buffering properties of hiPSC-CMs generated independently from multiple hiPSC lines.
- We directly compared Ca fluxes in hiPSC-CMs with primary Rabbit and mouse-CMs.
- We demonstrate that independently generated hiPSC-CM lines from healthy donors exhibit comparable and reproducible Ca handling and cytosolic Ca buffering properties.

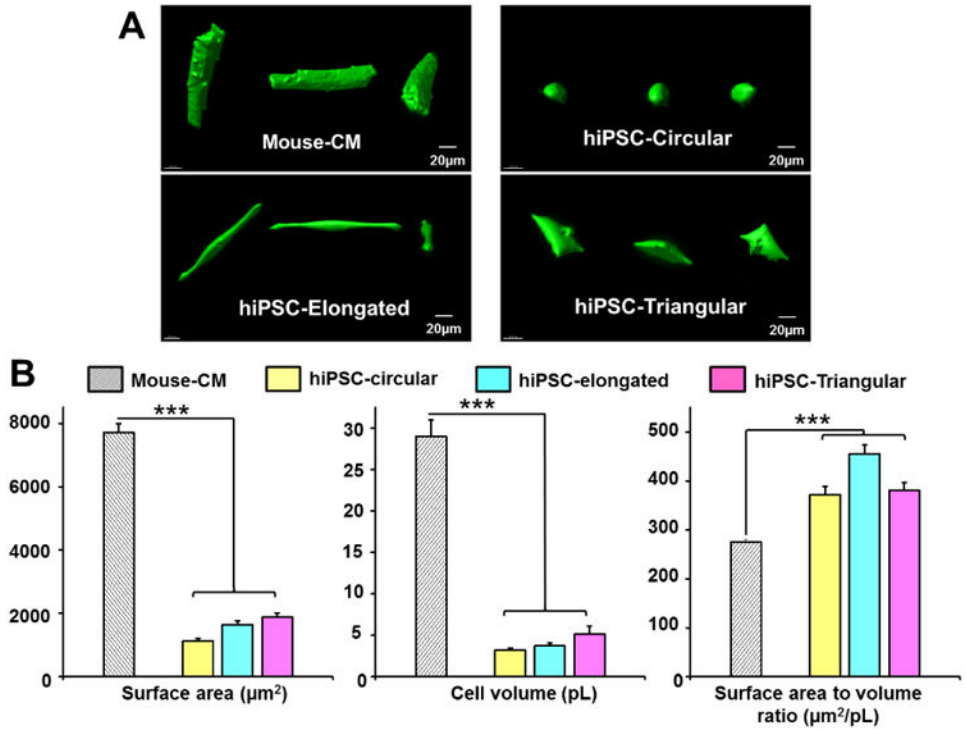

Fig. 1.

Surface area and volume of mouse-CM and hiPSC-CMs. A, representative examples of three-dimensional reconstruction of mouse-CM and hiPSC-CMs. B, averaged data. Values are mean±SEM. N=13-34 per group. ****P*<0.001 vs mouse-CM.

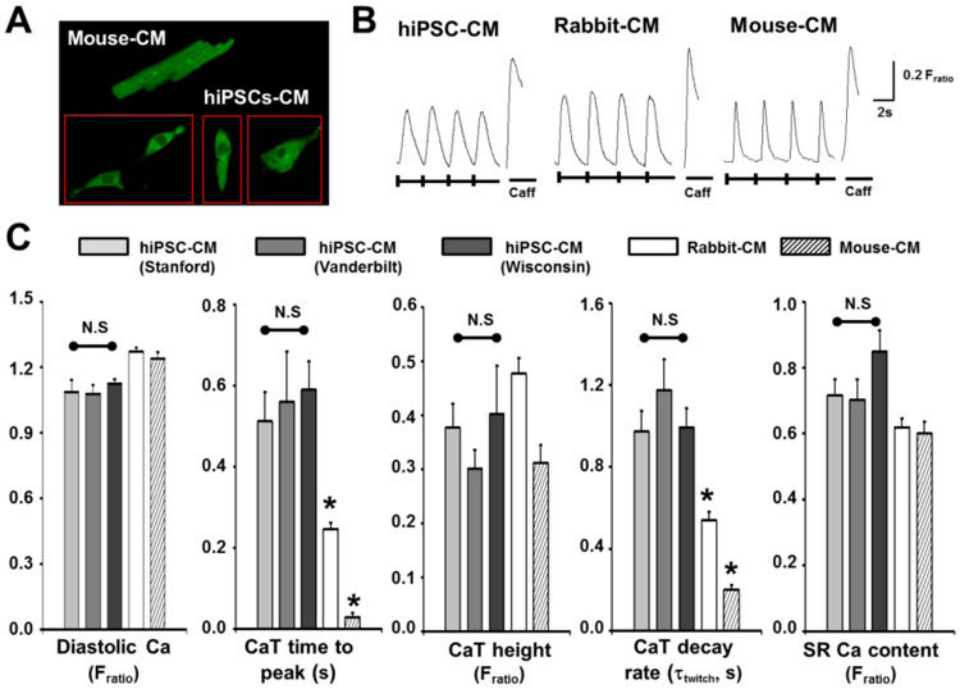

Fig. 2.

Ca handling of hiPSC-CMs and animal CMs. A, confocal images of a mouse-CMs and hiPSC-CMs loaded with low-affinity Ca indicator, Mag-Fluo-4 AM 5 μM to label intracellular Ca stores (i.e. SR). B-C, representative Ca transients (B) and averaged data (C) recorded in hiPSC-CMs and acutely isolated adult ventricular rabbit and mouse CMs. Cells were field-stimulated (0.5 Hz, 20 s train) in 2 mM Ca Tyrode's solution followed by caffeine spritz (10 mM, 5s) to estimate SR Ca content. Values are mean±SEM. N=22-27 per group. **P*<0.05 vs. hiPSC-CM. (hiPSC-CM images (A) and example Ca transient records (B) shown are from Vanderbilt hiPSC-CMs).

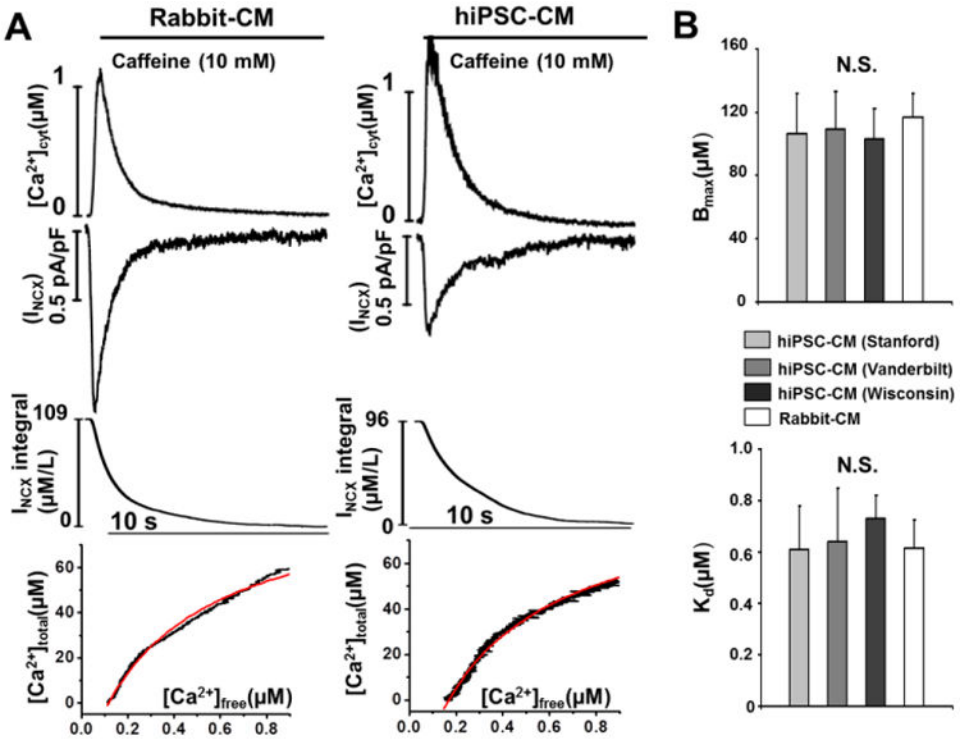

Fig. 3.

Cytoplamic Ca buffering properties of hiPSC-CMs and rabbit-CMs. A, representative cytoplasmic buffering curves generated using the Trafford method by plotting cytosolic $[ca]_{free}$ against the change in total cytoplasmic Ca concentration ($\Delta[ca]_{total}$) derived from the NCX current integral during caffeine spritz to release SR Ca in hiPSC-CMs (example trace from Stanford hiPSC-CM) and rabbit-CMs. B, averaged data. Values are mean±SEM. N=9-12 per group.

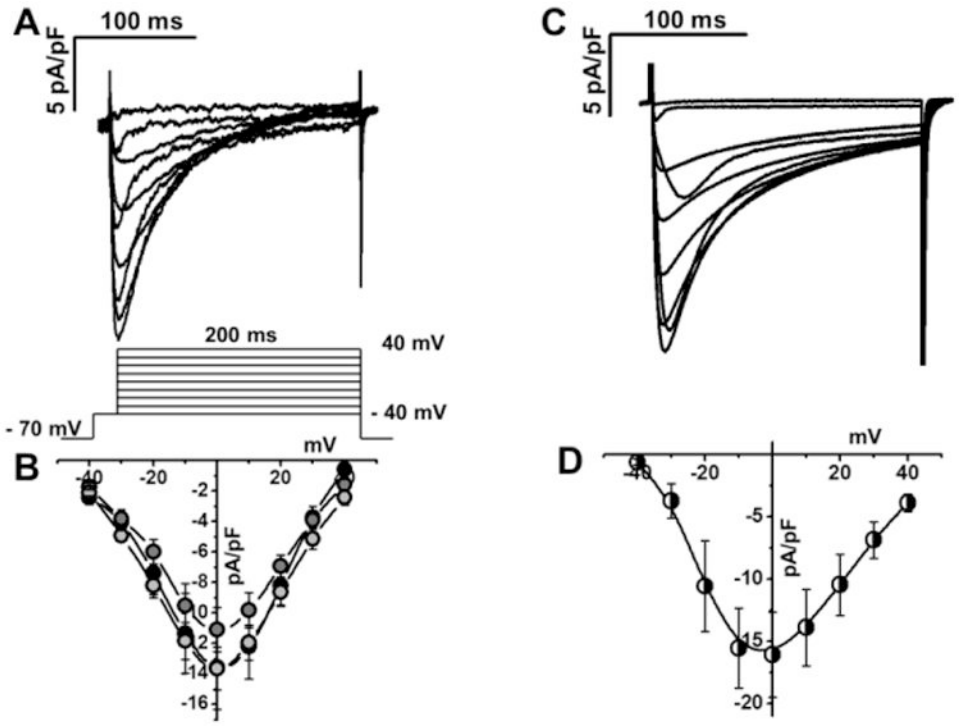

Fig. 4.

L-type Ca currents of hiPSC-CM and mouse-CM. A, C, representative example of Ca currents from hiPSC-CM (Stanford, A) and mouse-CM (B). Voltage protocol shown below current records. B, D current-voltage relationships of peak Ca currents from hiPSC-CM (Stanford, light gray, n=6; Vanderbilt, gray, n=6; Wisconsin, black, n=5) and from mouse CM (n=6), respectively.

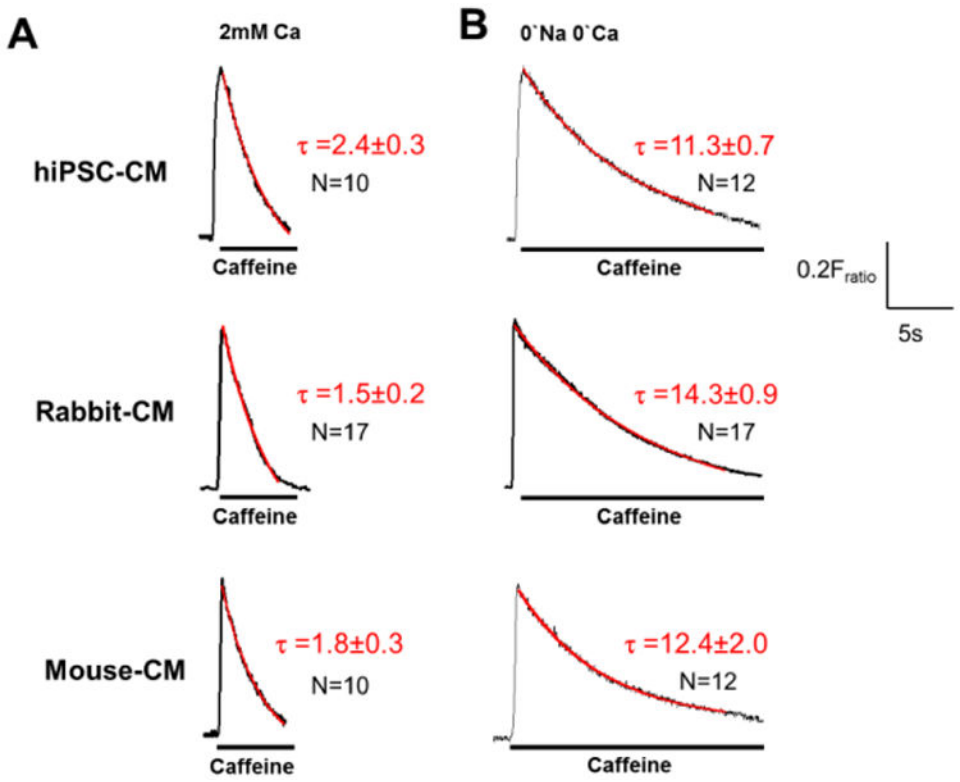

Fig. 5.

Measurement of NCX and non-NCX Ca efflux. A, hiPSC-CM (example trace from Wisconsin hiPSC-CM) and animal CMs were exposed to Tyrode's solutions containing 10 mM caffeine to measure combined NCX and non-NCX mediated Ca efflux. B, to measure only non-NCX-mediated Ca efflux, CMs were exposed to Tyrode's solution lacking Na and Ca. The Ca transient decay rate (τ) was calculated for each cell and averaged for each group. N= 10-17 per group. *P<0.05 vs. animal-CMs.

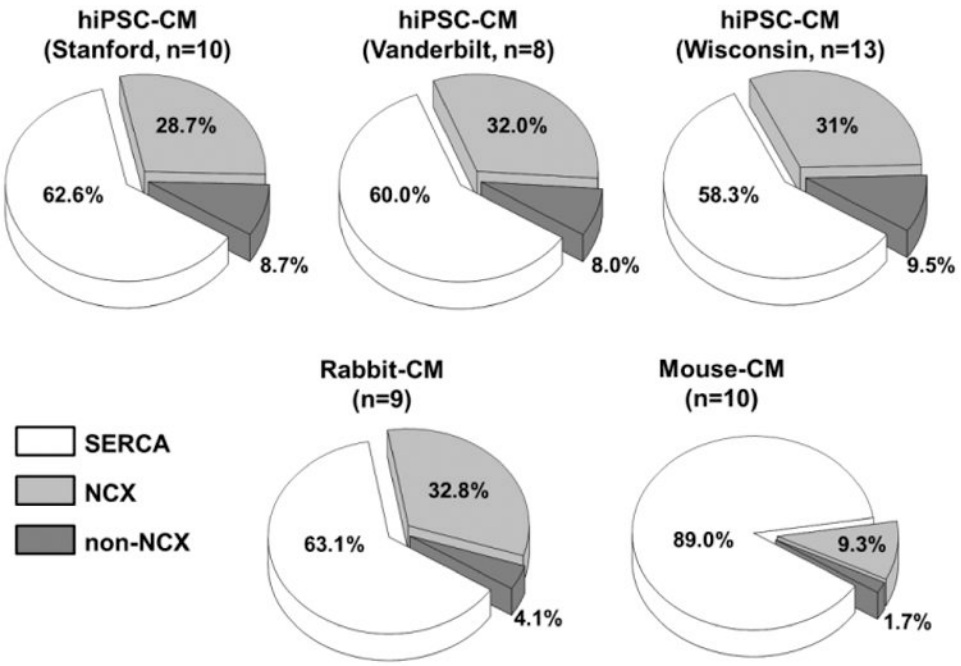

Fig. 6.

Relative contribution of Ca flux pathways in different CMs. K_{SERCA}, K_{NCX}, and $K_{non\text{-}NCX}$ were calculated from rate constants of decay of field-stimulated and caffeine-induced Ca transients (see supplemental table 1). The individual rate constants were normalized by total flux rate (K_{twitch}), yielding the relative contribution of Ca flux pathways for the three hiPSC-CM lines, rabbit-CMs and mouse-CMs.

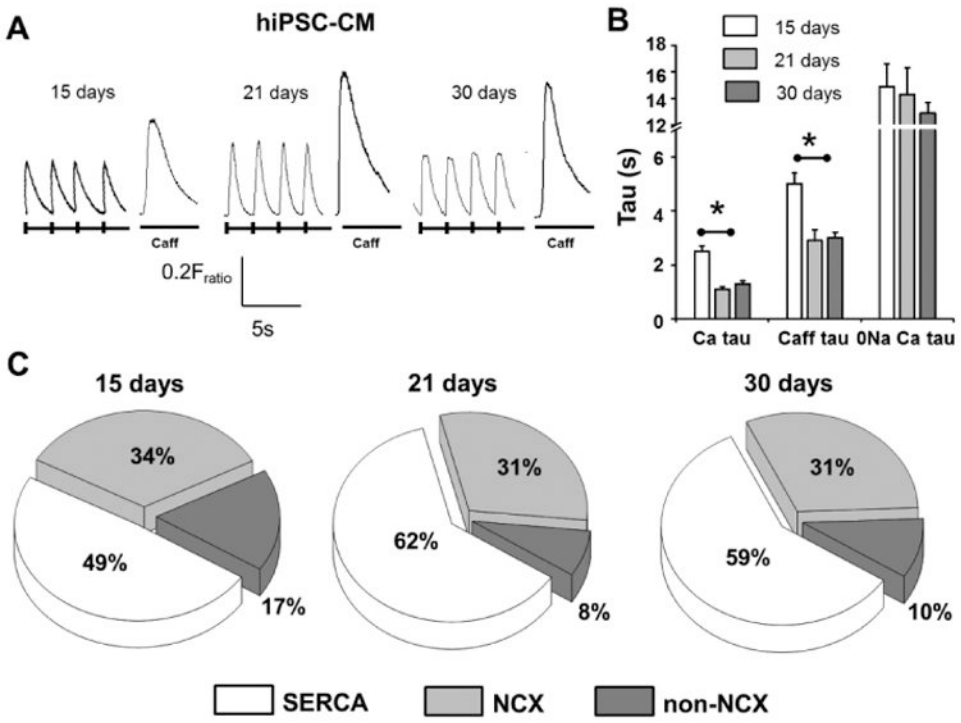

Fig. 7.

Maturation of Ca handling in hiPSC-CMs. A-B, representative Ca transients (A), and average data (B) of field-stimulated (τ_{twitch}) and caffeine-induced Ca transients (τ_{Caff}, $\tau_{Caff0Na}$) at day 15, 21, and 30 after hiPSC-CM induction. Data are from hiPSC-CMs generated at the University of Wisconsin. C, relative contribution of Ca fluxes calculated as in Fig. 5. N= 13-22 per group. *P<0.05 vs. 15 days.

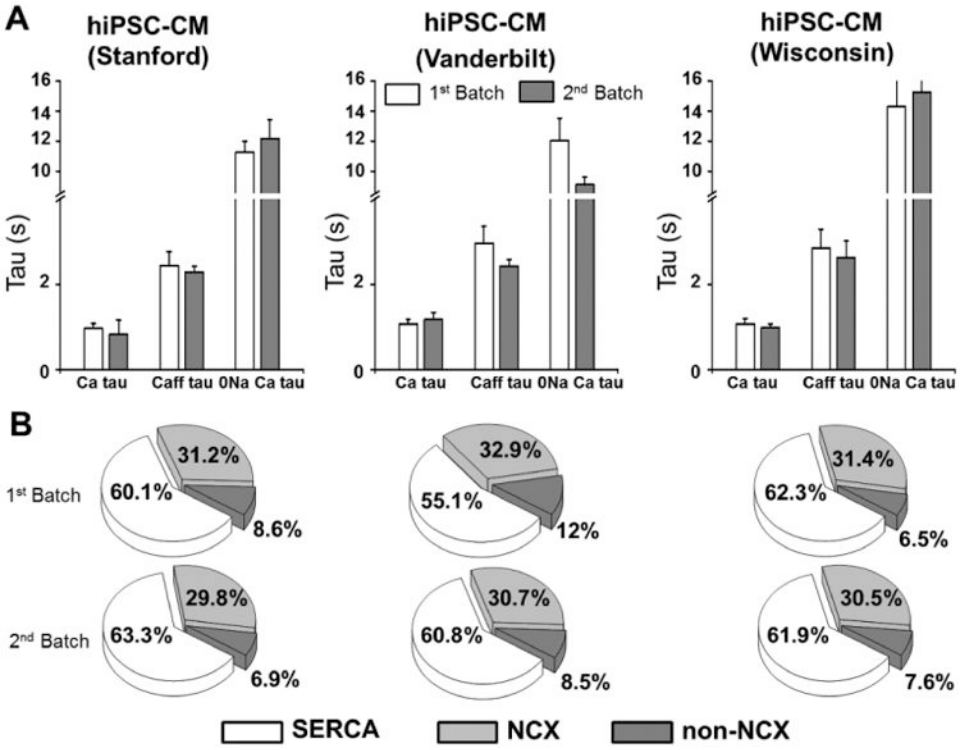

Fig. 8.

Reproducibility of Ca handling parameters in hiPSC-CMs. A, average data of field-stimulated (τ_{twitch}) and caffeine-induced Ca transients (τ_{Caff}, $\tau_{Caff0Na}$) from two independent platings of each hiPSC-CM line. Values are mean±SEM, N= 13-22 per group. B, relative contribution of Ca fluxes calculated as in Fig. 5.